Chapter 2

Synthesis of ZnS Nanoparticles using L-proline as Template, Their characterization and Application as asymmetric catalyst in Organic Transformation

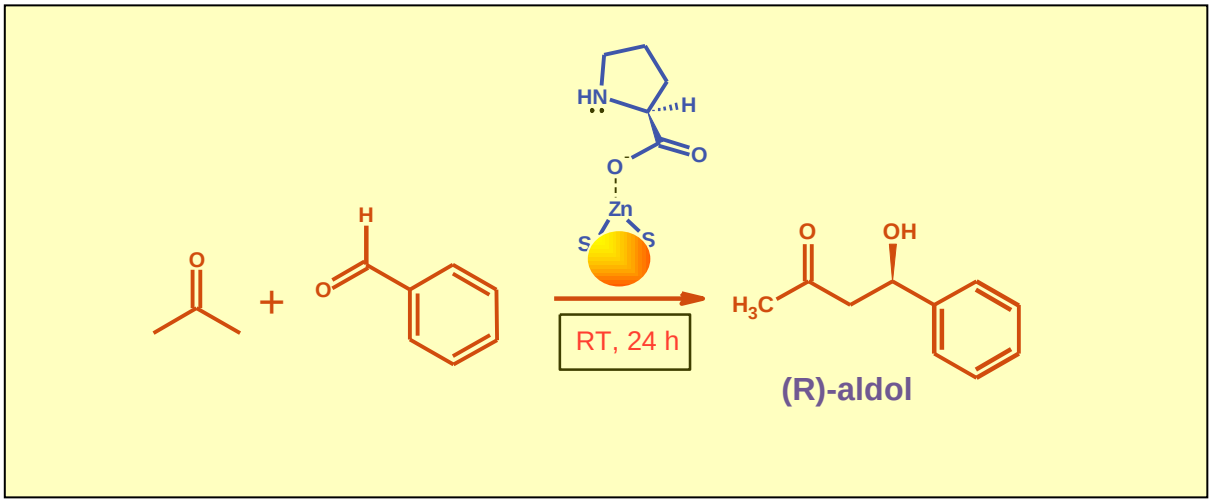

Inducing chirality on ZnS nanoparticles for asymmetric aldol condensation reactions

This study demonstrates that surface engineered, chirality induced, ZnS nanoparticles can be used as a catalyst for direct asymmetric aldol condensation reactions at room temperature.

Published in

***RSC Adv.*, 2013, 3, 17453-17461: DOI: 10.1039/C3RA41285G**

2.1. Introduction

Aldol condensation reaction is one of the classical organic reactions that has contributed progress in the field of catalysis and organic synthesis, particularly in the processes of C-C bond formation.[1, 2] Catalytic aldol reactions are also considered as a waste free method (100% atom economy) when carried out in presence of base or basic ion-exchange resins.[3]This reaction involves condensation between enolic and ketonic forms of same (self condensation) or different carbonyl compounds (cross condensation). The stereo selectivity of the process depends on the way in which the electron donor- acceptor species react but requires systematic strategies. The resulting products having desired stereochemistry is controlled by many factors such as temperature, pH, mole ratio of the reactants, thermodynamic and kinetic control, geometry of the reacting species, catalysis, chiral auxiliaries involved in the reaction, hydrogen bonding, interaction between solvent and reaction species etc.[4]For this purpose, different types of catalytic systems are developed with the progress of the field. Most of these are either enzymes[5,6] or non-transition metal Lewis acid (eg. tetramethylsilane (TMS), Lithium diisopropylamide (LDA), alkyl boranes).For example, B. List et al, in 1998, reported, Aldolase antibody 38C2 (Aldrich no. 47,995-0) catalyzes the aldol reaction between hydroxyacetone and aldehyde ***7*** to give dihydroxyketone ***8a*** in an enantiomeric excess (ee) >99% Scheme 1.1.[5]

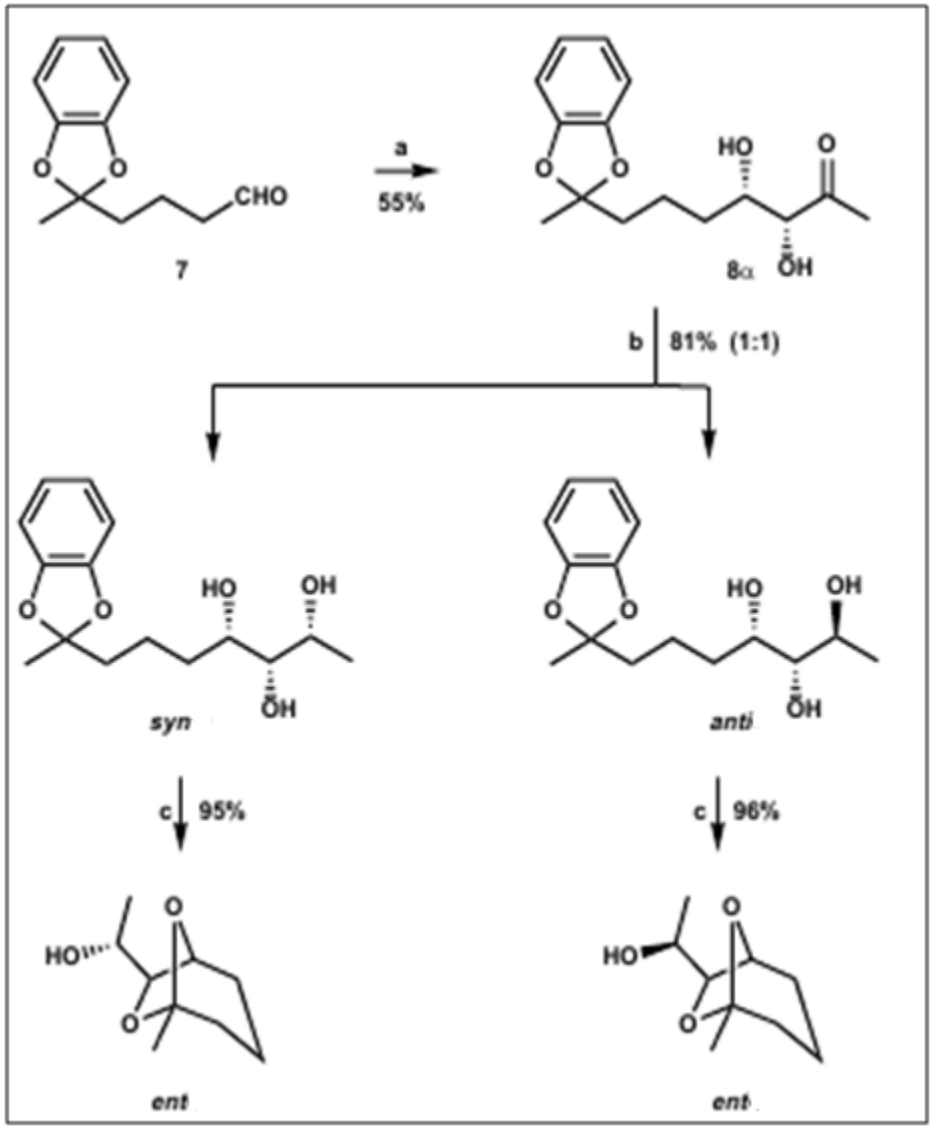

Scheme 2.1. a) Antibody 38C2 (0.66 mol %), hydroxyacetone (5 vol%), phosphate buffered saline (PBS, pH 7.4); b) $NaBH_4$, MeOH; HPLC separation; c) p-TsOH, C_6H_6 , 60 ^oC (Ref 5).

However, in recent years, transition metal and rare earth metal based complex compounds have also been reported as chiral catalyst for condensation of silylenol ethers with different aldehydes (the Mukaiyama reaction[7]) in aqueous media.[8]For example, Kobayashi et al reported copper (II) catalyzed Mukaiyama aldol reaction in an ethanol-water solution.

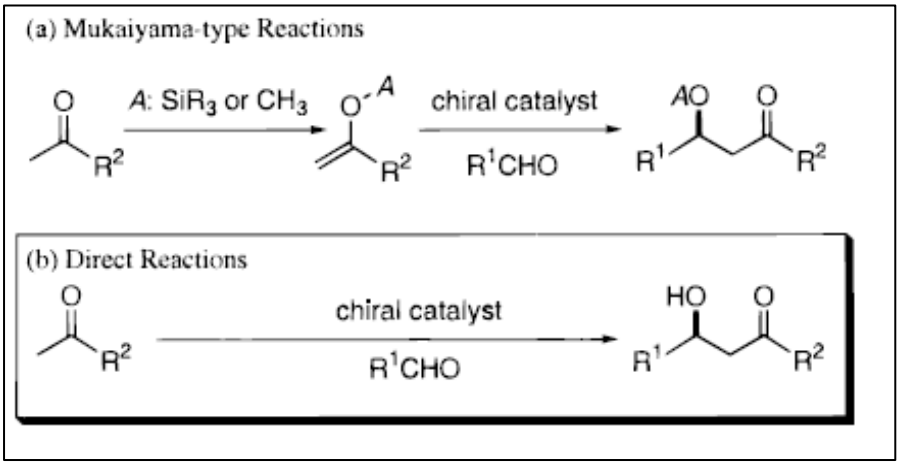

Scheme 2.2. Several Types of Catalytic Asymmetric Aldol Reactions.

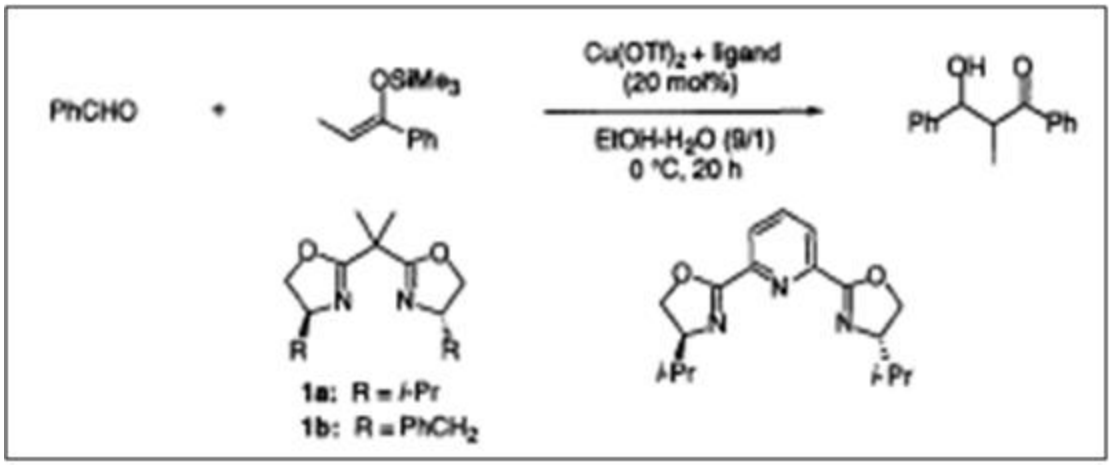

Scheme 2.3. The Mukaiyama reaction in aqueous media (Ref 8a).

In another work, the same author also reported the application of lanthanide (III) trifluoromethanesulfonate (particularly yitterbiumtriflate), a substitute for traditional Lewis acid, for Mukaiyama aldol reaction in presence of water. They reported that high yield and selectivity can be obtained at -15 to 0 ^{o}C in protic solvents like water. The same group of researchers also reported that Fe (II) and Fe (III) salts also exhibited a good activity for Mukaiyama aldol reaction in aqueous THF.[9]

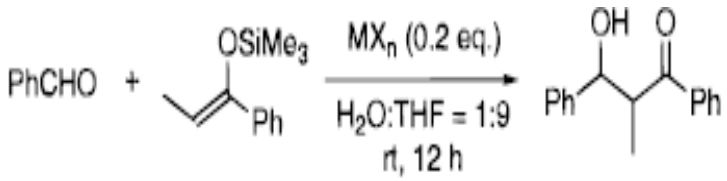

Scheme 2.4. Effect of Metal Salts in the Aldol Reaction (Ref 9).

Mlynarski and co-workers reported C_2-symmetric cationic aqua complex of Fe(II)-pybox (bis (oxazolinyl) pyridine) as an effective Lewis acid catalyst for the same reaction in aqueous media. They obtained aldol products in good yield and 70% enantioselectivity.[10]

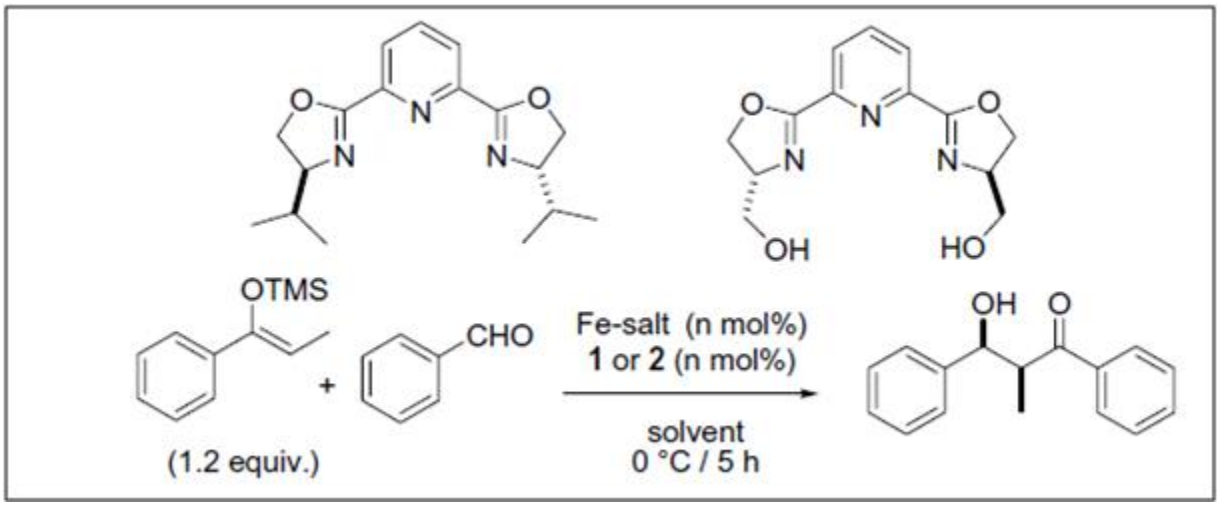

Scheme 2.5.Reaction of benzaldehyde with Z-enolsilyl ether 3 in presence of chiral iron(II)*pybox* (1)type catalyst (Ref 10).

Samarium diiodide and other lanthanide iodides are also very efficient Lewis acid catalyst for numerous reactions such as Mukaiyama aldol and Michael reactions. Several excellent reviews are available to discuss the state of the art in asymmetric aldol reaction. [8, 11]

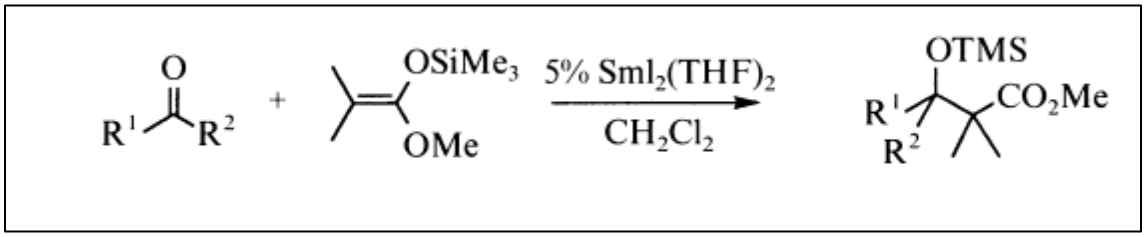

Scheme 2.6. Mukaiyama aldol reactions catalyzed by samarium iodides (P. Van de Weghe, J. Collin, *Tetrahedron Lett. ,* 1993, **3881**,34**).**

A few enantioselective aldolization processes involving Lewis base as catalyst have been reported. For example, Denmark et al. reported Lewis base chiral phosphor amide catalyzed asymmetric aldol addition of trichlorosilyl enolates.[12]

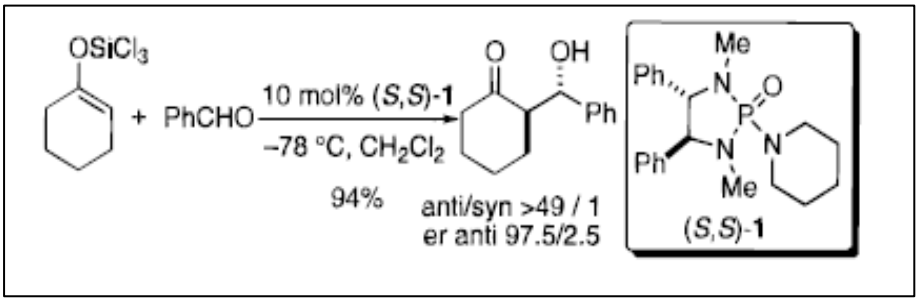

Scheme 2.7. Reaction through an organized, closed transition structure was borne out by the highly diastereo and enantioselective additions of geometrically defined trichlorosilylenolates of ketones catalyzed by the stilbenediamine-derived phosphoramide(*S,S*)-1 (Ref 12 a).

However, most of the above strategies involve homogenous catalysis. The benefits of heterogeneous catalysis[13]can be achieved if such 'microaldolase' type catalysts can be immobilized on some inert support or any other material which cannot only enhance the catalytic activity by coordinating with the original catalyst but also drive the reaction towards stereo specific pathway resulting products having high enantiomeric excess. Research activities in this direction have, however, been

scanty. List et al. first time reported the use of non-metallic small organic molecules like amino acids as catalyst for direct intermolecular asymmetric aldol reactions which opened a new avenue in the field of organo-catalysis.[14]

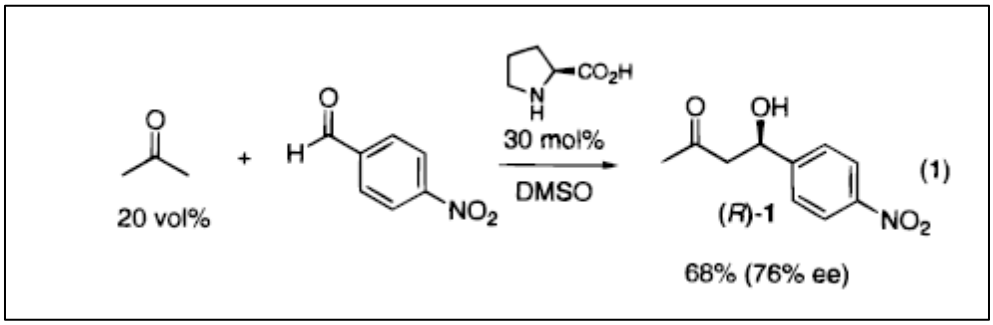

Scheme 2.8. Benjamin List et al (Ref 14) demonstrated the use of proline as a catalyst for the direct asymmetric aldol reaction between acetone and a variety of aldehydes.

Recently, Jing He et al. carried out aldol condensation between p-nitrobenzaldehyde and cyclohexanone using nanosheet (brucite type Layered Double Hyroxides of Zn and Al) attached α-amino acids (L-glutamic acid, L-aspartic acid, L-alanine and L-serine) as chiral ligands together with catalytic Zn^{+2} ions. They conclude, through theoretical optimization that such nanosheets not only sterically affects chiral induction in product but also assist in the formation of transition state via H-bonds.[15]Chiral auxiliaries like (R) and (S)-BINOL and other substituted enantio pure diols, were also used as additives for direct aldol reaction catalyzed by L-proline. Such bidentate additives coordinate with the catalyst L-proline and the aldehyde in appropriate orientation to facilitate the formation of

supramolecular transition state which in turn improve the enantioselectivity and rate of reaction.[16,17]

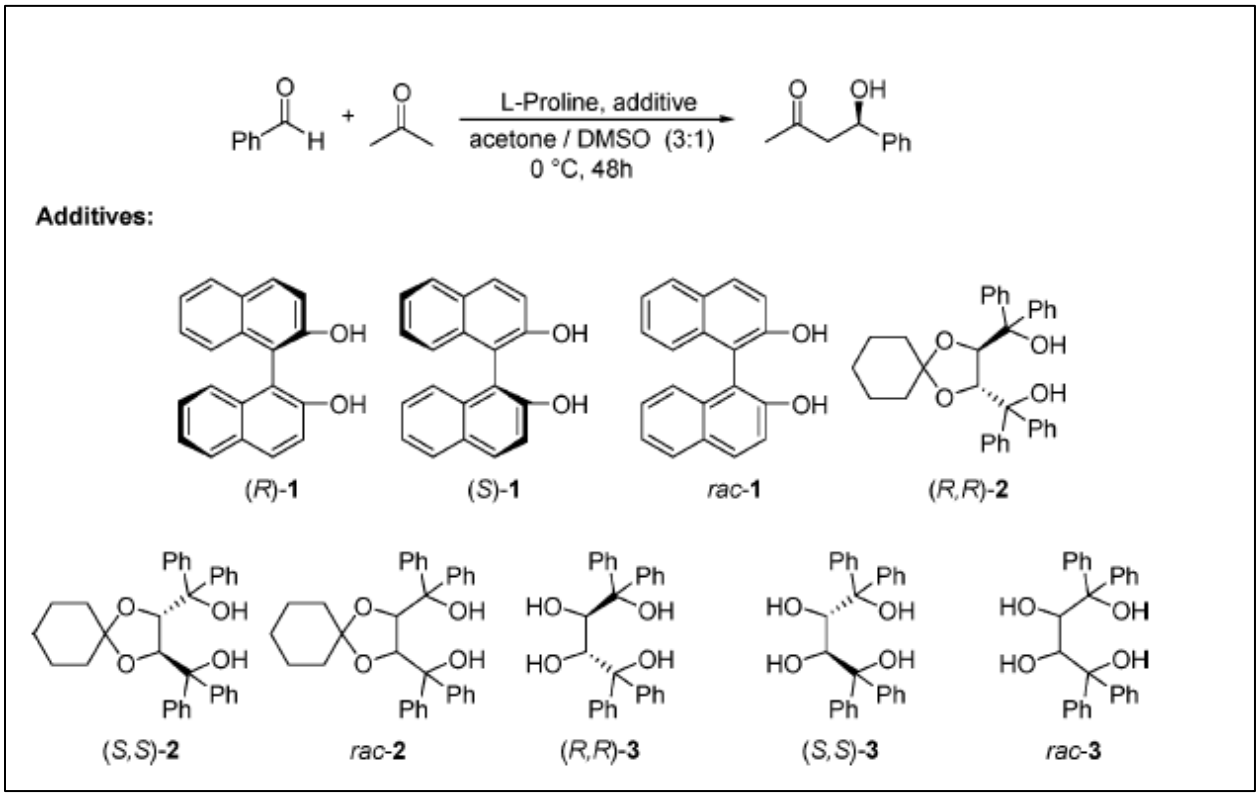

Scheme 2.9: Chiral auxiliaries evaluated for aldol reaction (Ref. 16)

Lakshmi Kantam et al. carried out direct asymmetric aldol reaction of aromatic aldehydes with acetone using nanocrystalline copper (II) oxide in presence of different chiral ligands such as substituted ethlylenediamine, (R) and (S)-BINAP, (+) and (-) - diethyl-L-tartarate etc. They obtained good to moderate enantioselectivity using different solvents such as THF, DMSO, $CHCl_3$ toluene etc. at different temperatures (25,0and -30^{o}C). They obtained optimum

enantioselectivity when toluene was used as a solvent at -30^{o}C (in 48 hours using 0.05 gm nano-CuO).[18]

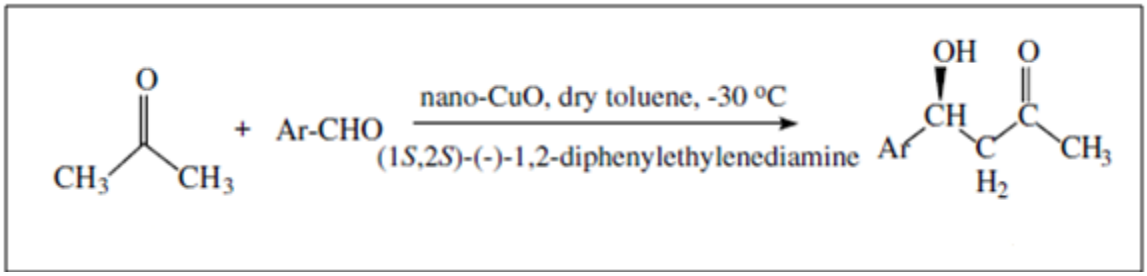

Scheme 2.10. Direct asymmetric aldol reactions of aromatic aldehydes with acetone using nanocrystalline copper(II) oxide (Ref 18).

Choudary et al., carried out aldol condensation between p-nitrobenzaldehyde and acetone catalyzed by aerogel prepared nanocrystalline MgO.[19] They achieved maximum enantioselectivity using THF as a solvent at -20^{o}C, under nitrogen atmosphere. In summary, increase in enantioselectivity with decrease in reaction rate was observed on lowering the temperature. However, maintaining such a low temperature may pose practical problems.

To improve stereo-selectivity, researchers are involved in developing various L-proline derivatives as potential catalyst for the direct intermolecular aldol reactions. For example, Tang, Z et al. developed L-prolinamides synthesized from L-proline and simple aliphatic and aromatic amines. They found these derivatives as active catalysts for the direct aldol reaction of p-nitrobenzaldehyde with neat acetone at room temperature (enantioselectivity upto 46% ee).[20]

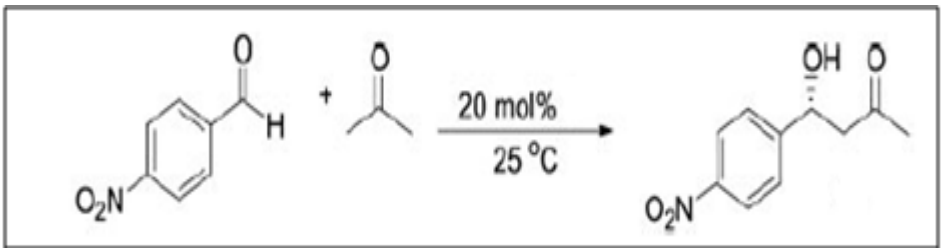

Scheme 2.11. Direct aldol reactions of 4-nitrobenzaldehyde with acetone catalyzed by various amide derivatives of L-proline-2 (Ref 20).

Table 2.1. Percent yield and percent enantiomeric excess obtained in aldol reaction in presence of different L-prolinamide derivatives (reported from Ref 20).

Entry	L-Prolinamide (2)	Yield,* %	ee,† %	Entry	L-Prolinamide (2)	Yield,† %	ee,‡ %
1	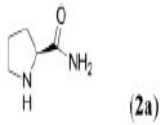 (2a)	80	30	7	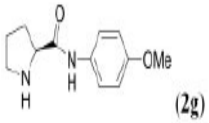 (2g)	78	31
2	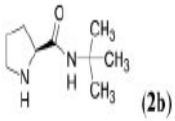 (2b)	55	15	8	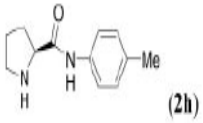 (2h)	80	34
3	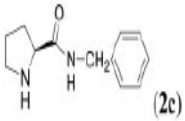 (2c)	82	21	9	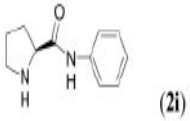 (2i)	88	37
4	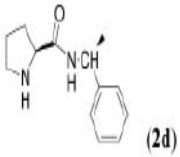 (2d)	64	15	10	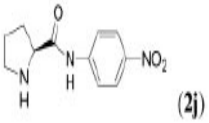 (2j)	80	39
5	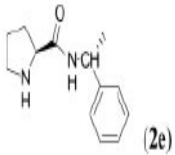 (2e)	63	23	11	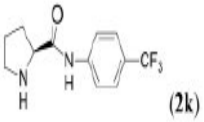 (2k)	88	45
6	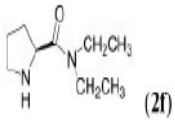 (2f)	71	18	12	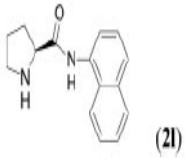 (2l)	82	46

*The reaction was carried out in neat acetone with a concentration of 0.5 M.†Isolated yield based on the aldehyde.‡The ee values were determined by HPLC and the configuration was assigned as *R* by comparison of retention time.

Longbottom and O'Reilly et al. prepared a range of co-polymers of styrene and L-proline functionalized styrene using reversible addition-fragmentation chain transfer polymerization (RAFT) techniques and explored their applications in supported catalysis. They found activity of the developed supported catalyst comparable to that of L-proline.[21]

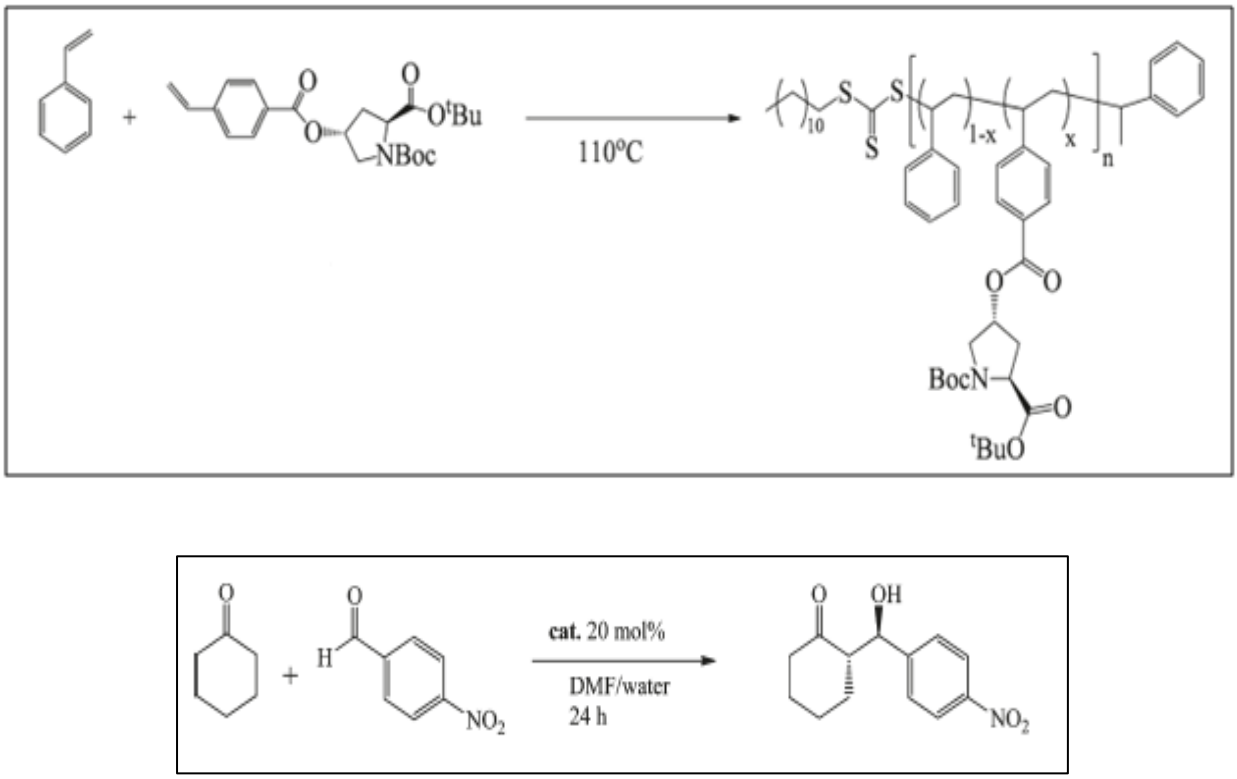

Scheme 2.12.Scheme representing bulk copolymerization of L-proline derivative with styrene using dodecyl 1-phenylethyl trithiocarbonate-3 as chain transfer agent to give copolymer *4* and aldol reaction carried out using this polymer as catalyst (Ref 21).

Joshi et al. carried out systematic evaluation of predesigned various L-proline derivatives modified either at α-hydrogen atom or at carboxylic acid group. It has been proposed that steric at the α-position effect adversely on the outcome of the direct aldol reaction.[22]

Above account suggests that optimum enantioselectivity can be achieved at very low temperature, using diverse and costly chiral auxiliaries and different solvents (eg. toluene:DMSO, 3:1 part to avoid the solubility problem).[16]From the environmental point of view, use of such solvents have their own drawbacks. Thus, environmentally benign and safe direct catalytic asymmetric aldol process without using any costly chiral auxiliaries is desirable. In the present work, we are reporting solvent free, direct aldol condensation using L-proline immobilized ZnS nanoparticles served as a support as well as heterogeneous catalyst at room temperature. The product obtained was found to be significantly pure and not require any further purification i.e. column chromatography or crystallization.

2.2. Experimental

2.2.1 Materials.

Zinc sulphate $ZnSO_4.7H_2O$, sodium sulphide $Na_2S.xH_2O$, ammonia and acetone were obtained from S.D Fine Chemicals, Mumbai, India and used as received. Benzaldehyde was obtained from Loba Chemie Mumbai, India. 1-Naphthaldehyde,

2-naphthaldehyde, p-nitrobenzaldehyde, p-tolualdehyde and L-proline were purchased from Sigma-Aldrich chemicals, Germany. p-Chlorobenzaldehyde and p-cyanobenzaldehyde were purchased from Spectrochem, India. All the chemicals were of AR grade and used without further purification. Freshly prepared aqueous solutions were used for the synthesis of ZnS nanoparticles.

2.2.2 Synthesis of ZnS nanoparticles.

ZnS nanoparticles were synthesized by co-precipitation method. In 50 mL aqueous solution of $ZnSO_4.7H_2O$ (0.03 mmol), ammonia solution was added dropwise until the pH of the solution stabilized to 10.To this solution, 25mL aqueous solution of L-proline(0.04mmol) was added and the temperature of the reaction mixture was gradually raised to 70^oC. The reaction mixture was stirred thoroughly for further half an hour to obtain homogenous mixture. To this solution, 25 mL Na_2S solution (0.05 mmol) was added dropwise at the rate of 1 mL/min. The reaction mixture was further stirred for 10 hrs to obtain homogeneous stabilized dispersion. Here, L-proline also acts as a capping agent stablizesgrowing ZnS nanoparticles and prevents aggregation. At the end, the reaction mixture was centrifuged at 10,000 rpm for 5 mins and subsequently washed with water and ethanol to remove impurities and traces of L-proline. The precipitates were dried at room

temperature. ZnS nanoparticles were also synthesized without L-proline (pristine ZnS) for comparison purpose maintaining the other experimental conditions same.

2.2.3 Aldol condensation reaction.

The as-synthesized ZnS nanoparticles (0.012 mmol) were suspended in acetone (0.08 mmol)and stirred for 15 mins. Benzaldehyde(0.04mmol) was subsequently added and mixture was stirred for about 24 hrs. At the end, the reaction mixture was centrifuged to remove the catalyst. The excess reagents were distilled out. The product (4-hydroxy-4-phenylbutan-2-one) was extracted with ethylacetate and dried with sodium sulphate. Ethylacetate was distilled to recover the product. The recovered catalyst L-proline / ZnS nanoparticles were washed with acetone and then again used for second and third cycle in similar manner. Similarly, recovered acetone was also utilized for the next cycles.

4-Hydroxy-4-(4'-nitrophenyl)butan-2-one. Reddish oil.IR (film)*v* /cm^{-1}: 3424 (broad), 1700, 1518, 1346, 1076, 747.^{1}H NMR (400 MHz, $CDCl_3$) δ (ppm): 2.23(s, 3H), 2.86 (m, 2H), 5.28 (m, 1H), 7.55 (d, 2H), 8.21 (d, 2H).^{13}C NMR ($CDCl_3$, 400 MHz) (ppm): 208.64, 128.85, 126.44, 124.3, 123.79, 68.90, 51.51, 30.76. Chromatography: *i*-PrOH/hexane (30:70), retention time - 6.09 min (major), 10.24 min (minor), 73 % ee. MS: [M+] m/z, found: 209.13; calculated ($C_{10}H_{11}NO_4$): 209.19.

4-Hydroxy-4-(4'-cyanophenyl)butan-2-one. Yellow solid.IR (pallet)*v* /cm^{-1}: 3427 (broad), 2227, 1712, 1503, 1362, 1075, 836.^{1}H NMR (400 MHz, $CDCl_3$) δ (ppm): 2.21 (s, 3H), 2.83 (m, 2H), 5.19 (m, 1H), 7.47 (d, 2H), 7.63 (d, 2H).^{13}C NMR ($CDCl_3$, 400 MHz) (ppm): 208.68, 148.13, 132.37, 126.36, 118.78, 111.24, 68.94, 51.56, 29.36. Chromatography: *i*-PrOH/hexane (30:70), retention time: 5.63 min (major), 6.46 min (minor), 83 % ee. MS: [M+] m/z, found: 189.11; calculated ($C_{11}H_{11}NO_2$): 189.21.

4-Hydroxy-4-(4'-chlorophenyl)butan-2-one. Light brown solid. IR (pallet)*v* /cm^{-1}: 3428 (broad), 1684, 1591, 1423, 1090, 760.^{1}H NMR (400 MHz, $CDCl_3$) δ (ppm): 2.22(s,1H), 2.83(m,1H), 5.15(m,1H), 7.28-7.35(m,4H).^{13}C NMR ($CDCl_3$, 400 MHz) (ppm): 209.07, 131.58, 128.90, 128.70, 127.04, 69.18, 51.78, 29.72. Chromatography: *i*-PrOH/hexane (10:90), retention time- 6.2 min (major), 8.4 min (minor), 81 % ee. MS: [M+] m/z, found: 198.63; calculated ($C_{10}H_{11}ClO_2$): 198.64.

4-Hydroxy-4-phenylbutan-2-one. Yellowish oil.IR (film)*v* /cm^{-1}: 3418 (broad), 1712, 1360, 1061, 755, 701.^{1}H NMR (400 MHz, $CDCl_3$) δ (ppm): 2.20 (s, 3H), 2.79-2.94 (m, 2H), 3.40 (d, 1H), 5.17 (m, 1H), 7.28-7.37 (m, 5H).^{13}C NMR ($CDCl_3$, 400 MHz) (ppm): 209.19, 142.76, 128.56, 127.70, 125.65, 69.84, 52.00, 30.80. Chromatography: *i*-PrOH/hexane (15:85), retention time- 4.4 min (major),

4.9 min (minor), 55% ee. MS: [M+] m/z, found:164.11; calculated ($C_{10}H_{12}O_2$): 164.201.

4-Hydroxy-4-(4-methylphenyl)-butan-2-one. Yellowish oil.IR (film) *v* /cm^{-1}: 3440 (broad), 1706, 1361, 1070, 819, 542.^{1}H NMR (400MHz, $CDCl_3$) δ (ppm): 2.20 (s, 3H), 2.35 (s, 1H) 2.77–2.93 (m, 2H), 3.33 (s, 1H), 5.12 (d, 2H), 7.17 (d, 2H) 7.26 (d, 2H).^{13}C NMR ($CDCl_3$, 400 MHz) (ppm): 209.21, 137.36, 129.73, 129.21, 125.60, 69.72, 52.02, 30.80, 21.12. Chromatography: *i*- PrOH/hexane (15:85), retention time- 4.4 min (major), 4.9 min (minor), 91 % ee. MS: [M+] m/z, found:178.14; calculated ($C_{11}H_{14}O_2$): 178.22.

4-(1-Naphthyl)-4-hydroxy-2-butanone. Yellow solid.IR (pallet)*v* /cm^{-1}: 3356 (broad), 1691, 1357, 1093, 795, 629.^{1}H NMR (400 MHz, $CDCl_3$) δ (ppm): 2.25 (s, 3H), 3.02 (m, 1H), 5. 98 (t 1H) 7.49-7.56 (m, 3H), 7.71 (d, 1H), 7.81 (d, 1H), 7.90 (m, 1H) 8.00 (m, 1H).^{13}C NMR ($CDCl_3$, 400 MHz) (ppm): 209.35, 138.18, 133.77, 129.86, 129.06, 128.13, 126.25, 125.6, 125.59, 123.00, 122.73, 66.68, 51.33, 30.82. Chromatography: *i*-PrOH/hexane (15:85), retention time- 7.8 min (major), 9.0 min (minor), 95 % ee. MS: [M+] m/z, found:214.22; calculated ($C_{14}H_{14}O_2$): 214.25.

4-(2-Naphthyl)-4-hydroxybutan-2-one. Yellowish oil.IR (film)*v* /cm^{-1}: 3415 (broad), 1710, 1361, 1071, 820, 749. ^{1}HNMR (400 MHz, $CDCl_3$) δ (ppm): 2.23 (s,

3H), 2.89-3.02 (m, 2H), 5.34 (m, 1H), 7.49 (m, 3H), 7.85 (m, 4H).^{13}C NMR ($CDCl_3$, 400 MHz) (ppm): 209.20, 140.07, 133.29, 132.95, 128.36, 128.00, 127.69, 126.25, 125.96, 124.37, 123.74, 69.97, 51.92, 30.85. Chromatography: *i*-PrOH/hexane (15:85), retention time- 9.0 min (major), 10.3 min (minor), 67 % ee; MS: [M+] m/z, found:214.00; calculated ($C_{14}H_{14}O_2$): 214.25.

2.2.4 Characterization of synthesized nanoparticles and Aldol products.

X-ray powder diffraction (XRD) pattern of the ZnS and L-proline /ZnS were obtained from X-ray powder diffractometer (Bruker D8 Advance) with Cu Kαradiation, λ=0.15418 nm. The L-proline/ZnS nanoparticles were dispersed in water, sonicated for 10 minutes, and then UV-Visible absorption spectra were recorded by means of Perkin-Elmer Lamda 35 UV-Visible spectrophotometer. Photoluminescence (PL) spectra were recorded on a Jasco FP-6300 spectrofluorometer using xenon lamp as the excitation source at 260 nm. The size and shape of the nanoparticles were studied by means of Transmission Electron Microscopy (TEM, Philips Tecnai 20). A BIC 90 plus (Brookhaven) equipped with 35.0 mW solid state lasers operating at 660 nm and an avalanche photodiode detector was used for the measurement of surface charges in term of zeta potential. The induction of chirality on the surface of Zns nanoparticles was confirmed by the measurement of absolute configuration using Circular Dichroism spectra recorded

on a Jasco, J-815 CD spectrometer. All measurements were made at 25 ^{o}C in DI water. The FTIR (Perkin-Elmer, RX-FTIR) spectra of the samples (catalyst and aldol products) were obtained in the range of 400 to 4000 cm^{-1}. The ^{1}H NMR and ^{13}C spectra of the aldol products were recorded on a Bruker Advance 400 MHz spectrometer using TMS as an internal standard in $CDCl_3$. All the synthesized aldol products were also analyzed by mass spectroscopy (ThermoScientific, DSQ-II) for structure confirmation. Optical rotations were measured by Jasco P-2000 polarimeter in terms of $[\alpha]_D$ (concentration c g/100 mL solvent). The absolute configuration (R) was assigned to the products by comparison of the optical rotation with the literature values.[14]Enantiomeric excess of all the products were determined by chiral HPLC analysis (Shimadzu, LC2010) by the method given in literature.[23]Chiralpak IA column (Daicel Chemical Industries Ltd) having dimension 250 x 4.6 mm and UV detector (254 nm) were used for the purpose. *i*-PrOH/ hexane in different proportion was used as mobile phase and 1.0 ml/min flow rate was maintained.

2.3. Results and Discussion

2.3.1 Compositional and morphological studies.

The XRD patterns of the as-synthesized ZnS nanoparticles are shown in Figure 2.1.

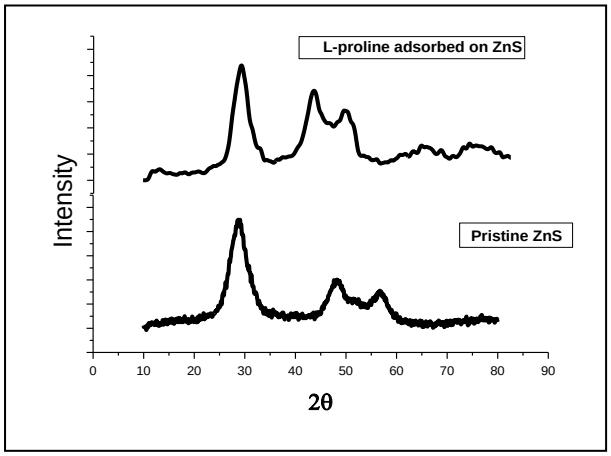

Figure 2.1. XRD Patterns of pristine ZnS and L-proline/ZnSNPs.

It can be seen that both the samples have similar XRD patterns and are matching with JCPDS card No. 65-0309, approving cubic zinc blende structure. The XRD patterns manifest three predominant diffraction peaks at 28.6°, 46.6° and 56.2° corresponding to the (111), (220) and (311) planes respectively. The nanoparticles are free from any impurities as no other major peaks were observed.The mean crystallite size, calculated using Debye-Scherrer formula ($L=0.9\lambda /\beta\cos\theta$) and FWHM (Full Width at Half Maximum) values corresponding to these planes was in the range of 8.3nm.[24] This observation indicates that there is no change in the phase of the ZnS before and after the adsorption of L-proline on the surface of nanoparticles. However, pattern of peaks correspond to (220) and (311) planes is little changed and shifted toward lower angles indicating electronic interaction of L-proline with surface planes of ZnS NPs.

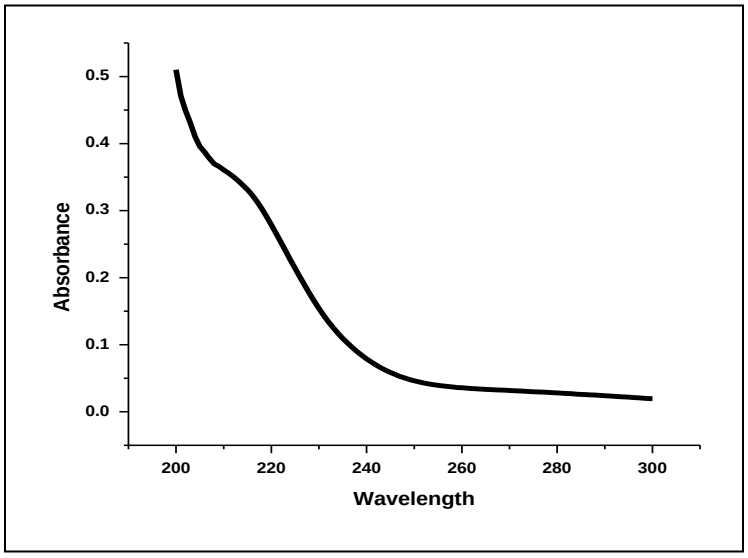

Figure 2.2: UV-Visible absorption spectrum of L-proline/ZnS NPs.

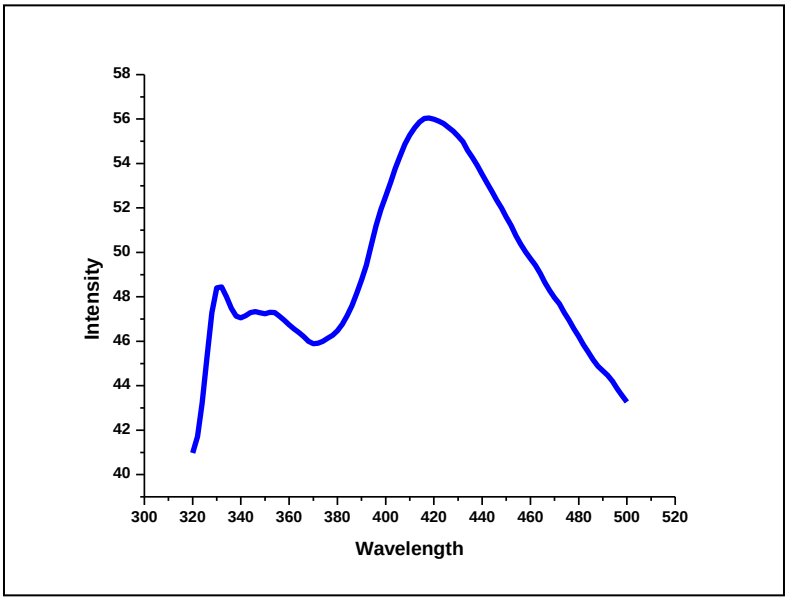

Figure 2.3.Photoluminescence emission spectrum of L-proline/ZnS NPs.

The quality of the pristine ZnS nanoparticles was further confirmed based on optical studies. As can be seen from Figure 2.2, the absorption edge at 217nm is due to band-edge transition in semiconductor NPs clearly indicates blue shift from

bulk value (345 nm), indicating quantum confinement and nano regime.[24]When suspended in ultrapure water and excited at 260 nm, sample luminesces at 435 nm (Figure 2.3). A strong peak in violet region at 330 nm is due to the defect sites (absence of Zn^{+2} or S^{-2} ions in ZnS lattice sites) in the sample. The defect sites cause radiative recombination processes between electrons (in conduction band) and holes (in valance band) resulting in a sharp intense peak.[26]The intense emission bands in blue region at 435 nm is due to sulfur vacancy and interstitial sulphur lattice defects.[27] The data show that sufficient sites are available to adsorb L-proline on the surface of nanoparticles. The size and shape of the nanoparticles were studied by TEM analysis (Figure 2.4).The TEM image of the L-proline capped ZnS nanoparticles shows almost monodisperse spherical particles with size ca. 2 nm.

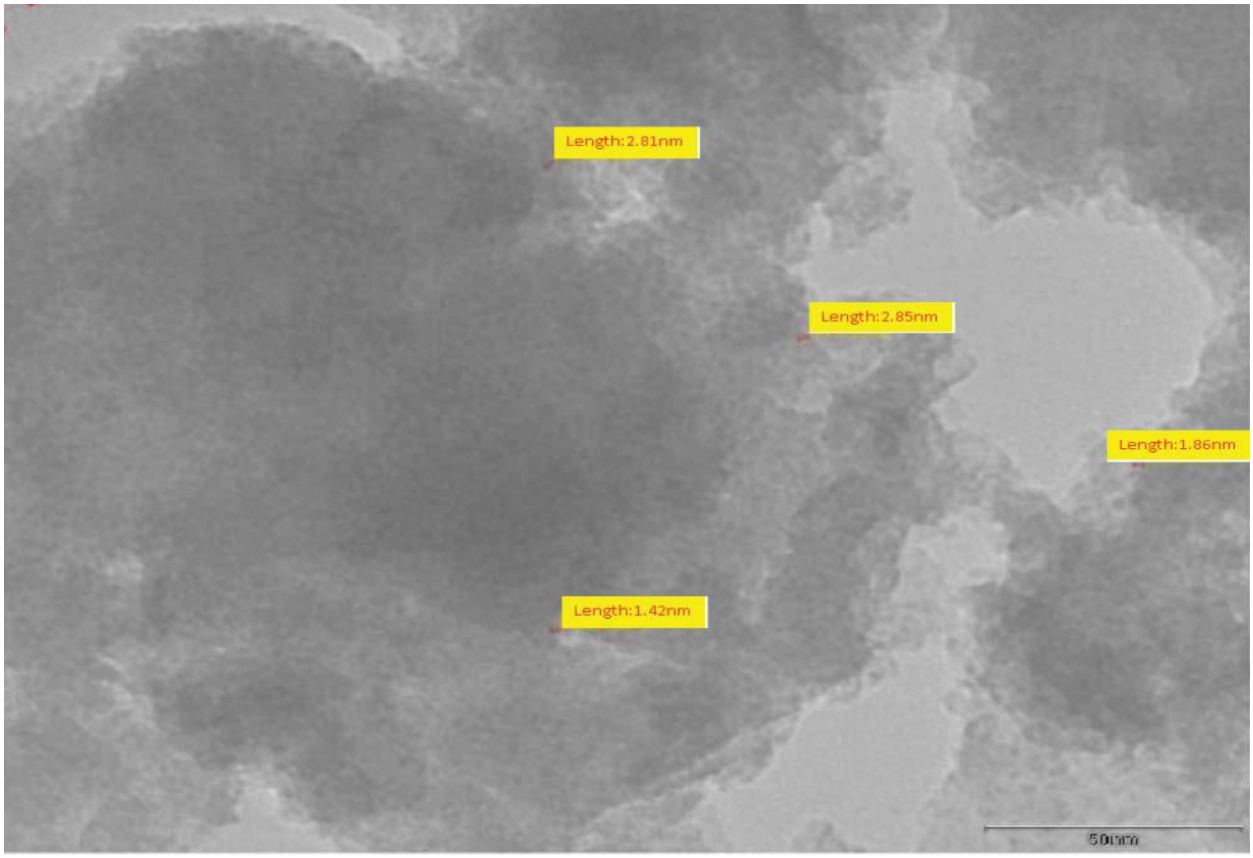

Figure 2.4.TEM image of L-proline /ZnS nanoparticles.

2.3.2 Immobilization of L-proline on ZnS nanoparticles.

ZnS is an ionic solid and semiconducting material of II-VI class with a band gap 3.8 eV. In the present strategy, ZnS /L-proline NPs have been developed as catalyst akin to α-Al_2O_3, zeolites and cationic clay sheets, could provide inert support to

α-amino acid molecules and/or it may also enhance the catalytic activity of

L-proline synergistically by surface coordination with the catalyst.[28, 29] It can definitely stabilize the transition state of the reaction even if it does not directly involve in catalysis. The catalytic activity and surface area of the material can be increased to many folds at nano regime and these parameters can be easily tuned by adjusting particle size together with the electrostatic charge. At the beginning, the pH of the reaction medium was adjusted to 10 by NH_3 but later it dropped down to 8.3 on addition of Na_2S, which remained same till the end of the reaction. L-proline exists in anionic form in basic medium and also acts as a capping ligand for growing ZnS nanoparticles. It adsorbs on the surface of nanoparticles and restricts their further growth. This results in a decrease in ζ value of ZnS nanoparticles (-30 mev in case of pristine ZnS nanoparticles to -15 mev for

L-proline /ZnS nanoparticles). L-proline can coordinate with surface Zn^{+2} ions by carboxylate group. Here, two possibilities arise;either L-proline coordinates bidentately with surface Zn^{+2} ions i.e. two oxygen atoms of carboxylate group coordinated or it may coordinate monodentately i.e. only one of the two equivalent oxygen atom interacts with surface ions (Figure 2.5).

To understand the interaction among the ligands and surface of the growing NPs, FTIR is one of the best tools. The mode of interaction of carboxylate ion present in anionic L-proline can be confirmed from vibrational spectroscopy (FTIR,

Supporting Information). Two characteristic absorption bands of carbon-oxygen vibrations can be observed in the region of 1700-1300 cm^{-1}.[30] One is an asymmetric -coo- stretching ν_{as}(coo) and other a symmetric -coo- stretching ν_s(coo). The characteristic major vibrational frequencies for pristine ZnS and

L-proline /ZnS nanoparticles are given in Table (supporting information).

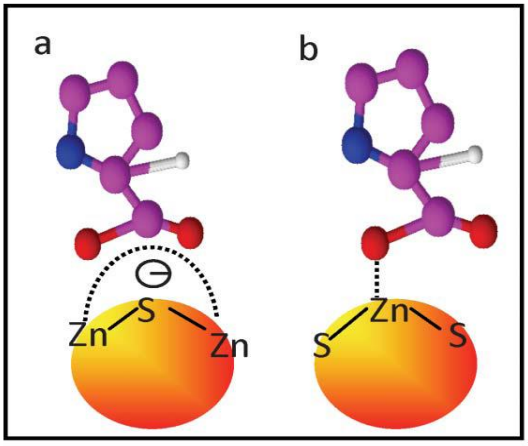

Figure 2.5. Mode of interaction of L-proline with the surface of ZnS NPs. (Orange balls indicate ZnS NPs, Purple for carbon atoms that of red oxygen and white hydrogen).

On comparing $\Delta(\nu_{as}(coo)-\nu_s(coo))$ with $\Delta'(\nu'_{as}(coo)-\nu'_s(coo))$, we found $\Delta<\Delta'$, (where Δ indicates difference in absorption bands for pristine ZnS while Δ' indicates the same for L-proline /ZnS) which suggests monodentate coordination of L-proline with ZnS surface.[31, 32] The shape and size of the nanoparticles show considerable effect on the adsorption of ligand. The preference of monodentate adsorption over bidentate indicates the prevalence of edge/corner defect sites and larger surface area. Moreover, on adsorption of L-proline on pristine ZnS, the

bands beyond 3400cm^{-1} became sharp and smooth, indicating the favorable alignment of ligand molecules on the surface of nanoparticles. The shift in the position of the bands shows good coordination between ligand and surface ions (Figure 2.6).[33]The change in the zeta potential value on adsorption of L-proline on ZnS NPs also corroborates this observation.

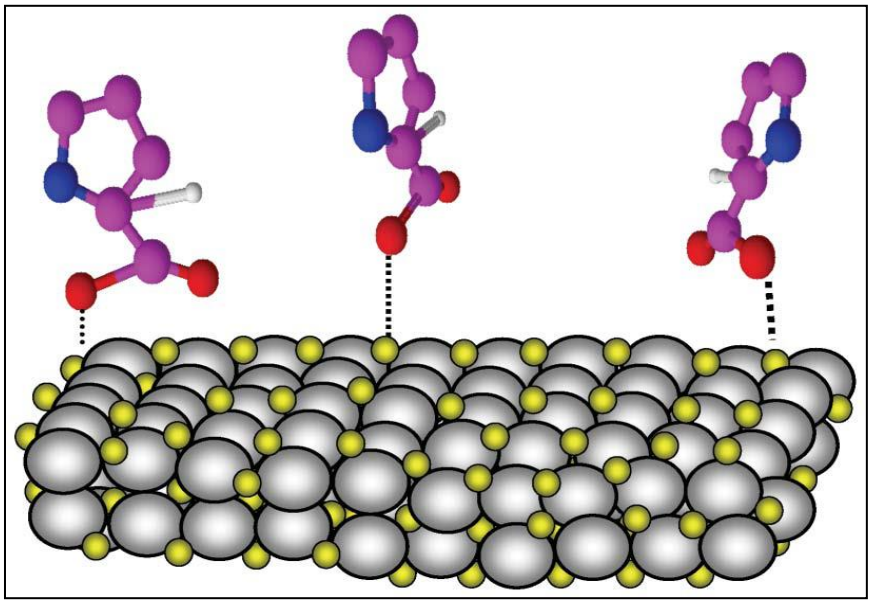

Figure 2.6.Zn^{+2} Coordinated L-proline on the surface of ZnS NPs.

= Zn^{+2} ions; S^{-2} ions

(Purple balls show carbon atoms that of red oxygen and white hydrogen).

2.3.3 Aldol condensation reaction.

The immobilized L-proline on ZnS NPs was used as catalyst in direct aldol condensation reaction under neat conditions. Generally, β-hydroxy aldehydes (aldols) or β-hydroxy ketones (ketols) are formed at the end of aldol reaction (aldolization) which in turn, dehydrate to yield α,β-unsaturated aldehydes or ketones (aldol condensation). We selected several aromatic and aliphatic aldehydes for comparison and condensed them with acetone (Claisen-Schmidt

condensation) in presence of developed catalyst in different sets of reaction (Table 2.2 and Scheme 2.13).

Sr.No	Aldehyde	Product	Reaction time (hrs)	Yield (%)	Enantiomeric excess* (%)

Table 2.2. Yields and ee of Aldol products with different aldehydes.

1	p-nitrobenzaldehyde	4-Hydroxy-4-(4'-nitrophenyl)-butan-2-one.	36	77	73
2	p-cyanobenzaldehyde	4-Hydroxy-4-(4'-cyanophenyl)-butan-2-one	24	75	83
3	p-chlorobenzaldehyde	4-Hydroxy-4-(4'-chlorophenyl)-butan-2-one	36	69	81
4	Benzaldehyde	4-Hydroxy-4-phenyl-butan-2-one	36	68	55
5	p-tolualdehyde	4-Hydroxy-4-(4-methylphenyl)-butan-2-one	48	67	91
6	1-naphthaldehyde	4-(1-Naphthyl)-4-hydroxy-2-butanone	48	70	95
7	2-naphthaldehyde	4-(2-Naphthyl)-4-hydroxy-2-butanone	48	75	67
8	p-hydroxybenzaldehyde	No reaction	-	-	-

9	Isobutyraldehyde	No reaction	-	-	-
10	t-butyraldehyde	No reaction	-	-	-

** Calculated from chiral HPLC.*

In this study, acetone was used as a solvent as well as a reactant. In earlier studies, DMSO, formamide or THF were employed as co-solvent to improve the solubility of L-proline in acetone.[14, 15, 16] However, DMSO has its own environmental problems. Due to its high boiling point (189 °C), it evaporates slowly at normal atmospheric pressure. The work-up procedure at the end of reactions involving DMSO is tedious as it cannot be easily recovered and it is very difficult to remove all traces of DMSO by conventional rotary evaporation. Recently, it was found that DMSO waste disposal into sewers can cause environmental odor problems in cities, waste water bacteria transform DMSO under hypoxic (anoxic) conditions into dimethyl sulfide (DMS) that is slightly toxic and has a strong disagreeable odor.[34, 35] Same problems are also encountered in case of THF and formamide.

However, in our study, being immobilized on ZnS nanoparticles, L-proline was suspended in the reaction mixture without using any co-solvent. Initially, we selected benzaldehyde to condense with acetone at room temperature for 24 hours and it furnished aldol product (R)-4-Hydroxy-4-phenylbutan-2-one with 68 % yield and 55 % enantiomeric excess. Its optical rotation was found to be $+26^{o}$ (c=1.1, $CHCl_3$). Comparision of the optical rotation with the literature value [14]

suggests that catalyst only favors the (R) aldol as the major product with the exclusion of reactions like dehydration, self-condensation,[36] 1,3-dipolar cycloaddition[37] etc. In order to test the stability of ZnS supported L-proline catalyst under repeated catalytic cycles, the same aldol reaction was carried out using recovered reactants compensated with fresh and recycled catalyst for three repeated cycles. Results are summarized in Table 2.2. It was found that there is no drastic change in $[\alpha]_D$ and % yield of the reaction for initial two cycles. However, 10% loss of % yield was observed for third catalytic cycles. This might be due to leaching of the catalyst from the surface.

Table 2.2.Yields and ee's of Aldol product of benzaldehyde at the end of different cycles.

Cycle	$[\alpha]_D$	Yield %	Enantiomeric excess	Enantiomeric ratio
I	$+26^o$ ($c=1.1, CHCl_3$)	68	63.26	4.4573 : 1
II	$+25^o$ ($c=1.1, CHCl_3$)	65	60.82	4.11:1
III	$+21^o$ ($c=1.1, CHCl_3$)	58	51.09	3.089:1

Synthesis of other aldol using L-proline /ZnS is reported in Table 2.2. The absolute configuration of all aldol products has been assigned on the basis of optical rotation[14] and chiral HPLC analysis with Chiralpack AI column.[23]

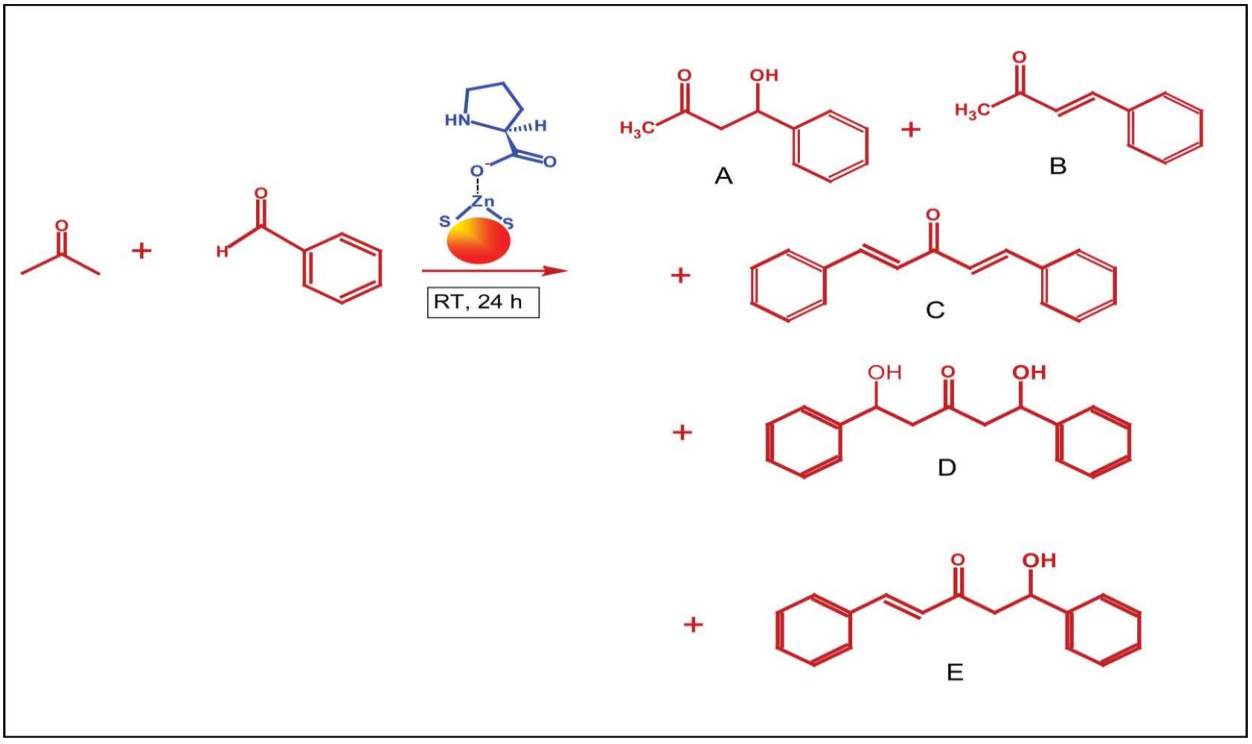

Scheme 2.13. Asymmetric direct aldol condensation reaction in presence of L-proline /ZnS NPs and possible products. Only product 'A' in (R)-configuration is favored.

2.3.4 Mechanism Investigation.

Many studies on enamine based mechanism of the same reaction under different condition proposed that L-proline acts as 'aldolase' type catalyst.[14, 38, 39, 40] In the present study, we propose the same mechanism, however, in this case surface zinc ions facilitate the catalytic activity of L-proline by acting as Lewis acid and providing coordination sites to the leaving group (Scheme 2.15).[15, 38]This supported enamine is electrophilically attacked by benzaldehyde. Here, the orientation (1) is preferred due to steric reasons. If the same reaction is carried out by homogeneous catalysis using L-proline only, the carboxylic proton of L-proline would have been

transferred to the carbonyl group of aldehyde forming alkoxide via six-membered transition state. In the present study, the same proton may be provided by the surface zinc ion coordinated hydroxyl group. In the formation of transition state, the carbonyl group of aldehyde preferred to orient in such a way that H-bonding among carbonyl oxygen, Zn coordinated hydroxyl group's surface proton and electron rich $-CH_2$ group facilitated. The stabilized transition state, in turn, favors orientation (1) rather than (2) due to steric reasons. The tricyclic H-bonded network support enantiofacial selectivity resulting in the formation of (R) product (Scheme 2.15).[14]

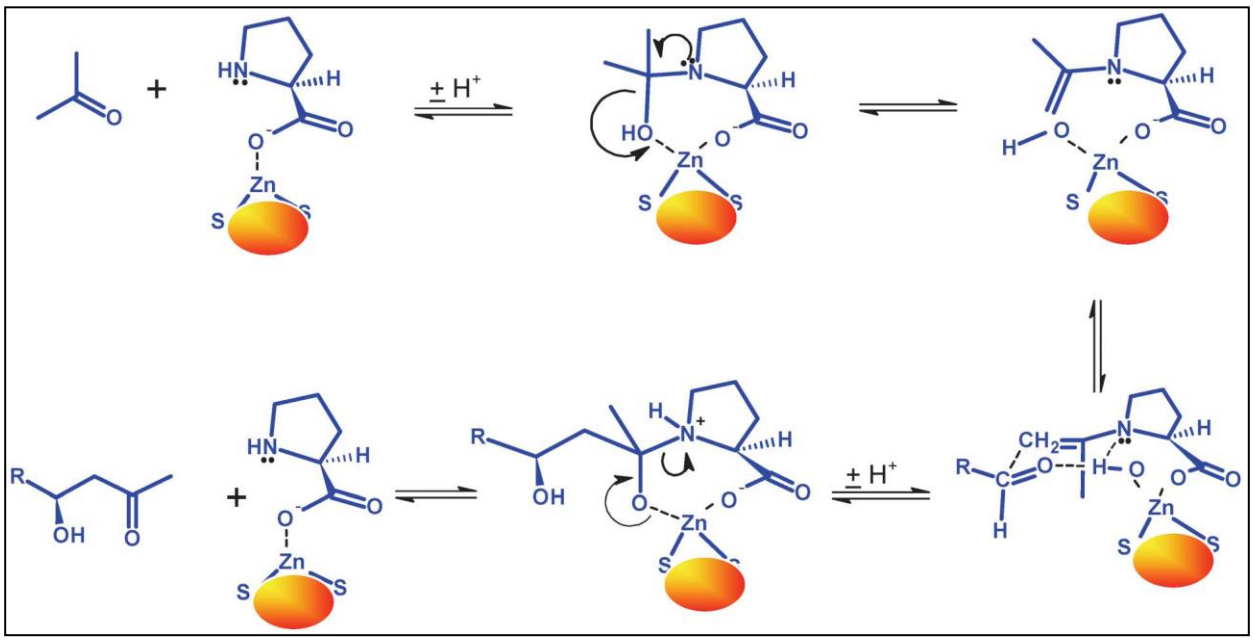

Scheme 2.14. Proposed reaction mechanism showing mediation of ZnS surface coordinated L-proline as a catalyst. Orange balls indicate ZnS NPs.

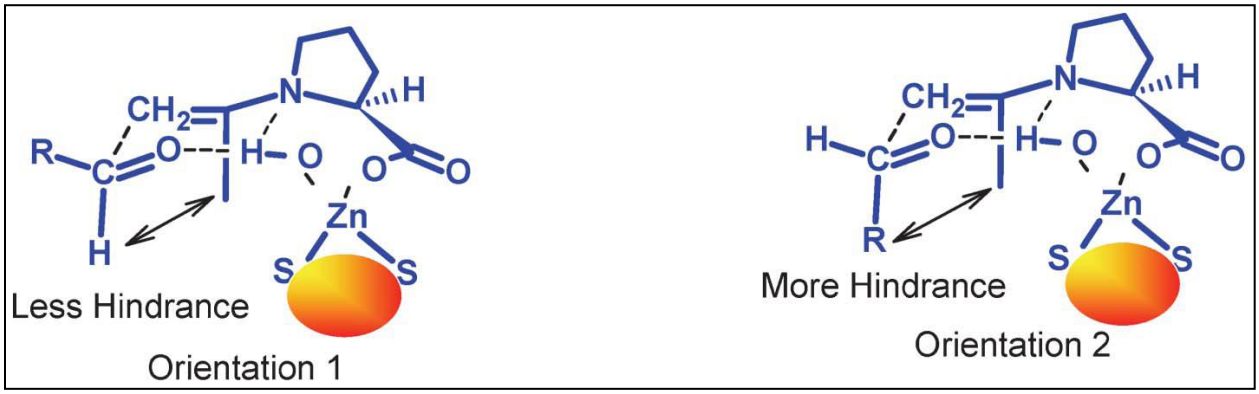

Scheme 2.15. Proposed transition states in different orientations of aldehyde. Orange balls indicate ZnS NPs.

We had carried out the same reaction with different aromatic aldehydes listed in the Table 2.1 to investigate the effect of bulky group on the transition state and selectivity of the product. Table 2.1 indicates that in all the case the (R)-aldol is preferred over (S)-aldol, suggesting the involvement of carbonyl group to form H-bonding with the hydrogen of Zn coordinated hydroxyl group and keeping the aromatic part away from the transition state resulting in (R)-aldol in enantiomeric excess. Generally, % ee is controlled by steric factors while % yields of a reaction by electronic factors affecting the stability of a transition state. It is interesting to observe that p-hydroxybenzaldehyde did not undergo aldol condensation with acetone while p-nitrobenzaldehyde gave maximum yield under the same reaction conditions. As hydroxyl group is stronger electron-releasing group, weakens the

positive charge on carbonyl carbon not sufficient to be attacked by nucleophile (acetone). To confirm further, we had selected aromatic aldehyde with less electron-releasing groups at para position, ($–CH_3$). We found that this aldehyde gave moderate yield. In case of p-nitrobenzaldehyde, $-NO_2$ group is electron-withdrawing, which strengthens the H-bond between carbonyl oxygen and Zn coordinated hydrogen, in turn, stabilize six-membered transition state and optimum yield was obtained. To support the argument, another aromatic aldehyde with electron-withdrawing group (-CN) at para position was selected. For this case, also, optimum yield was obtained. To further investigate the reactivity, different aliphatic aldehydes (isobutyraldehyde and t-butyraldehyde) were selected to undergo an aldol condensation with acetone under the same reaction conditions using L-proline/ZnS NPs. We found that these aldehydes did not undergo any reaction even after 24-30 hrs at room temperature. This observation can also be explained by diminishing electrophilicity of carbonyl carbon due to electron-releasing group. Out of benzaldehyde, 1-naphthaldehyde and 2-naphthaldehyde, the later gave maximum yield. This study leads to believe that aromatic ring, substituted or unsubstituted plays an important role both sterically and electronically to orient the reactants and stabilize the transition state resulting into a product with definite configuration.

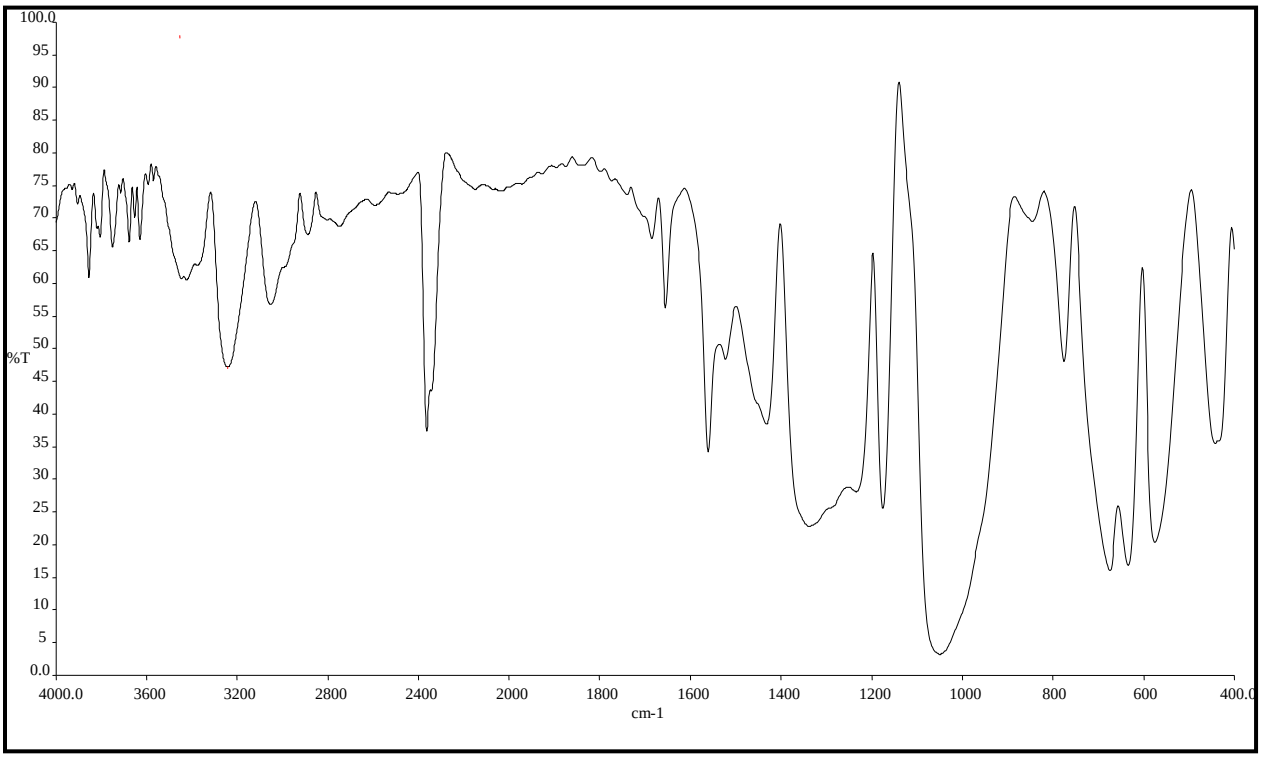

Figure 2.7(a). FTIR of L-Proline

Band Assignment

Sl. No.	**Wave numbers cm^{-1}**	**Band assignments**	**Sl. No.**	**Wave numbers cm^{-1}**	**Band assignments**
1	3012	υ_{as}CH2	12	1242	υC-O
2	2978	υ_{as}CH2	13	1189	τCH2
3	2969	υCH	14	1090	Γring
4	2956	υsCH2	15	1025	Γring
5	2938	υsCH2	16	950	γOH
6	1645	υC=O	17	907	Γring
7	1544	δNH	18	866	Γring
8	1446	δCH2	19	850	ρCH2

9	1375	δOH	20	799	ρCH2
10	1320	τCH2	21	721	δC=O
11	1292	δCH	22	630	Δring

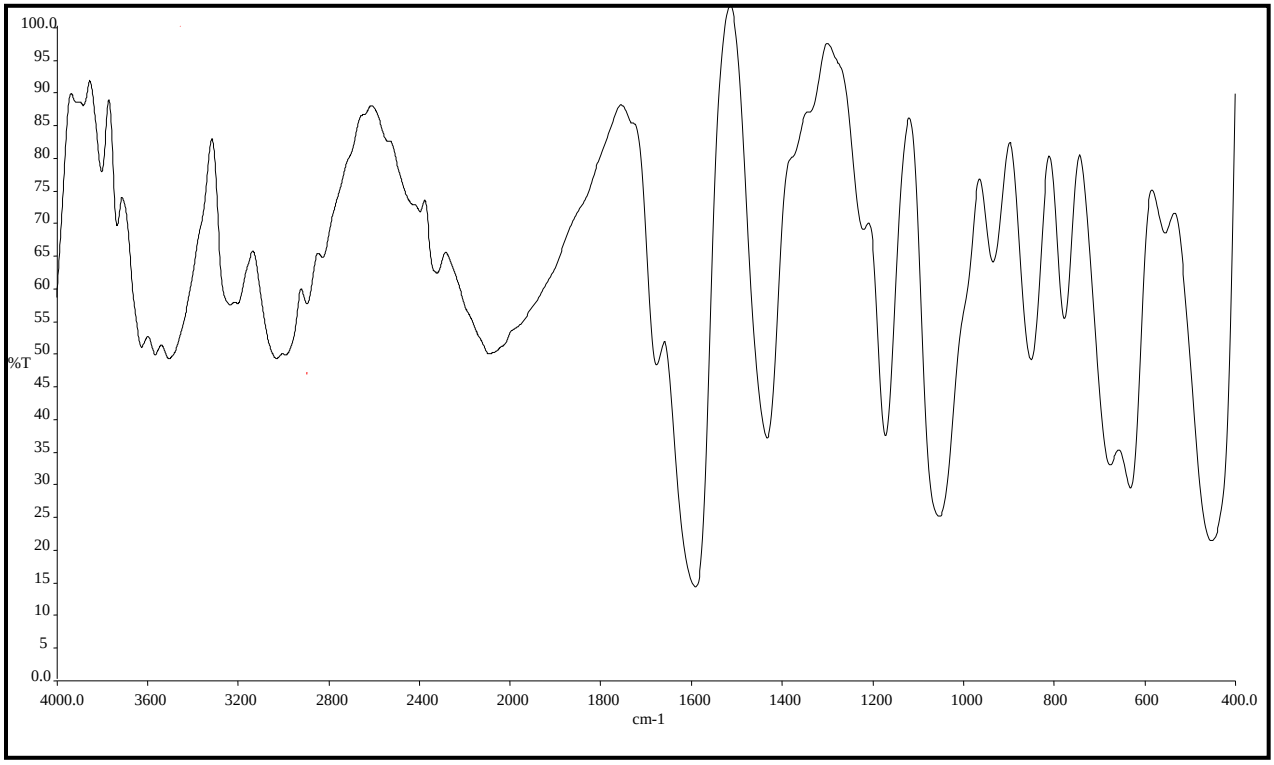

Figure 2.7 (b). FTIR of L-proline/ZnS

Band Assignment

Sl. No.	**Wave numbers cm^{-1}**	**Band assignments**	
1	3015	Asymmetric stretching	CH_2
2	2943	Asymmetric stretching	CH_2
3	2903	Symmetric stretching	CH_2
4	1661	Stretching	C=O
5	1552	In-place bending	NH
6	1392	In-place bending	OH
7	1331	Twisting	CH_2
8	1281	In-plane bending	CH
9	1153	Twisting	CH_2
10	1038	Stretching	Ring
11	946	Out of plane bending	OH
12	844	Rocking	CH_2
13	671	Stretching	Zn-S
14	636	In-plane bending	Ring
15	551	Stretching	Zn-S

CD spectra were recorded on a Jasco, J-815 CD spectrometer.

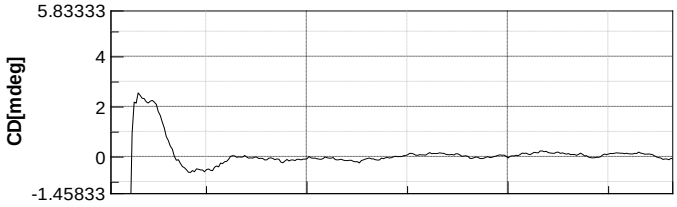

Figure 2.8(a). CD Spectra of undoped L-Proline adsorbed ZnS nanoparticles.

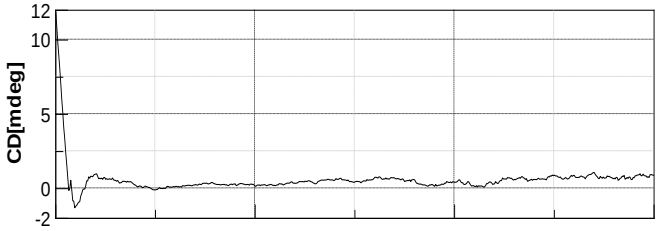

Figure 2.8(b). CD Spectra of undoped D-Proline adsorbed ZnS nanoparticles

NMR of 4-Hydroxy-4phenylbutan-2-one

After one recycle

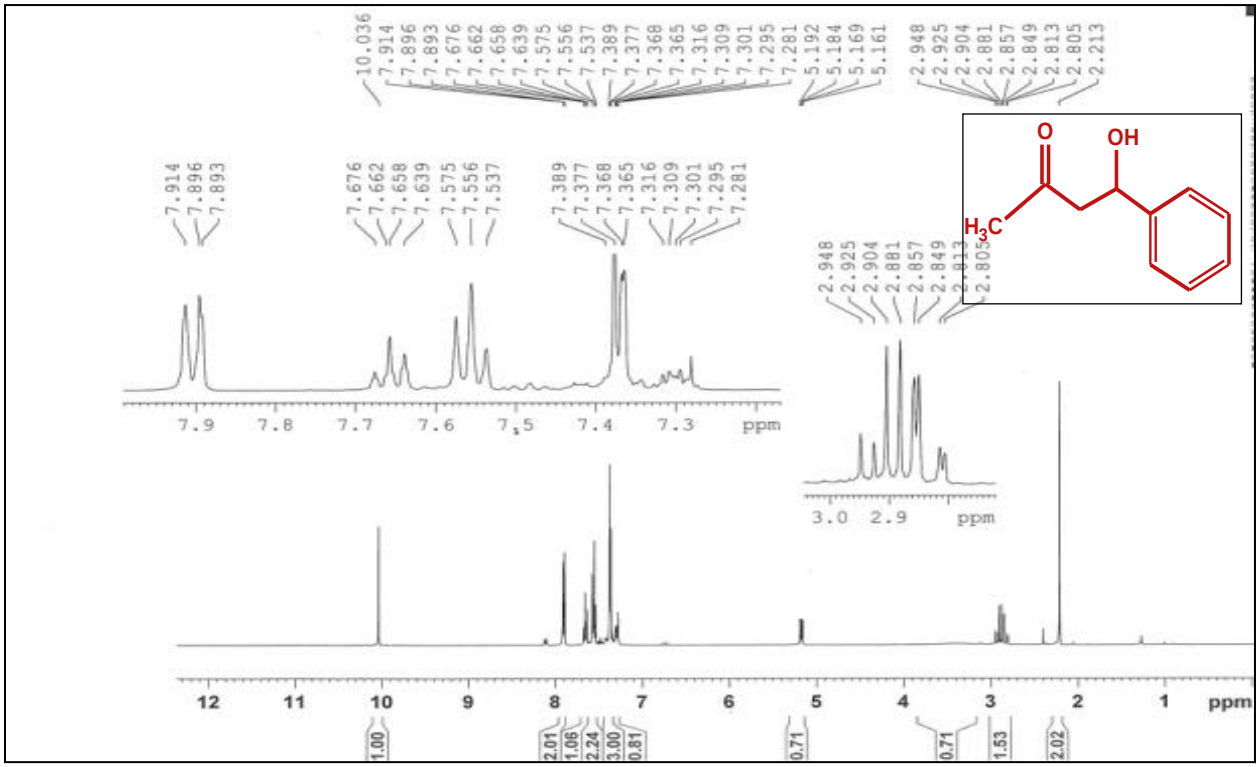

Figure 2.9(a): NMR of 4-Hydroxy-4phenylbutan-2-one

NMR of 4-Hydroxy-4phenylbutan-2-one

After third cycle

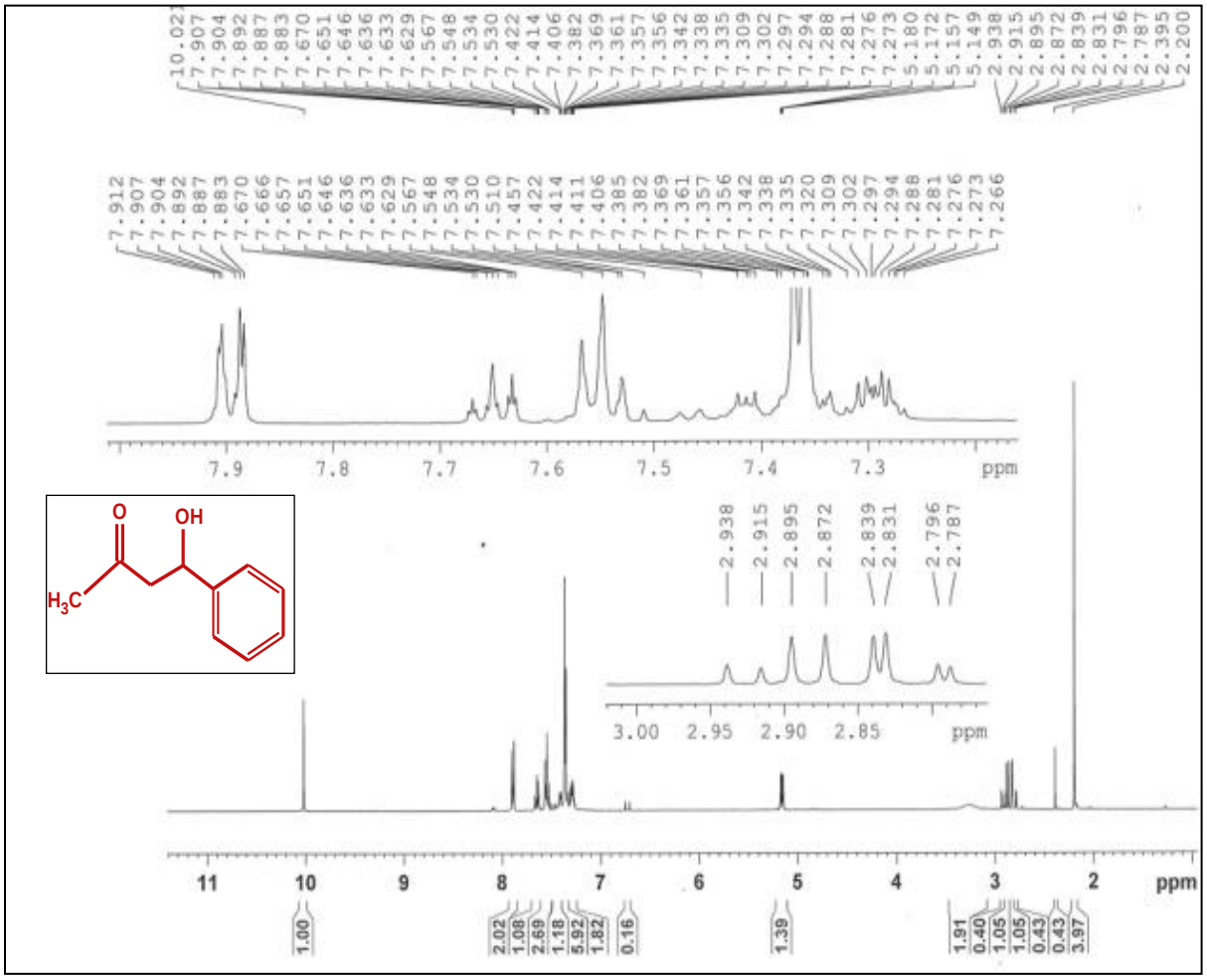

Figure 2.9(b). NMR of 4-Hydroxy-4phenylbutan-2-one

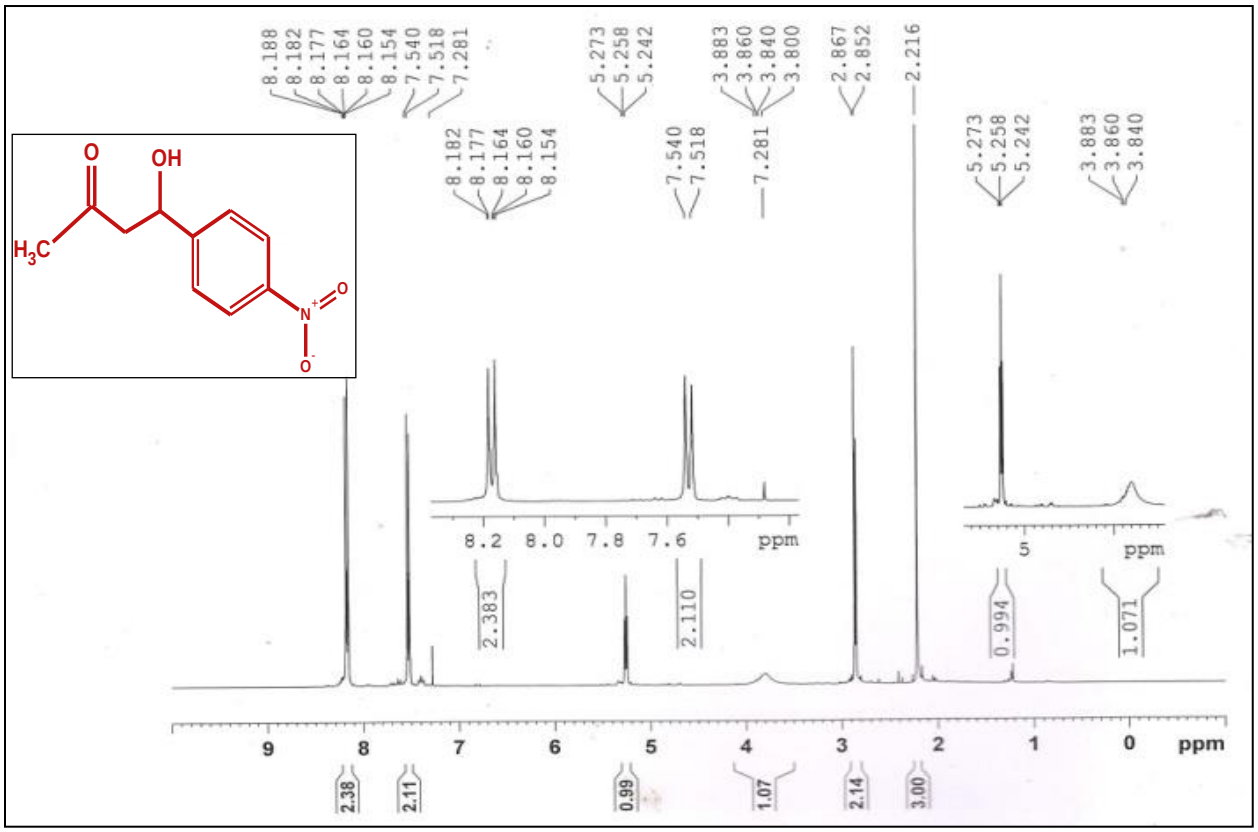

Figure 2.9(c). NMR of 4-Hydroxy-4-(4'-nitrophenyl)butan-2-one

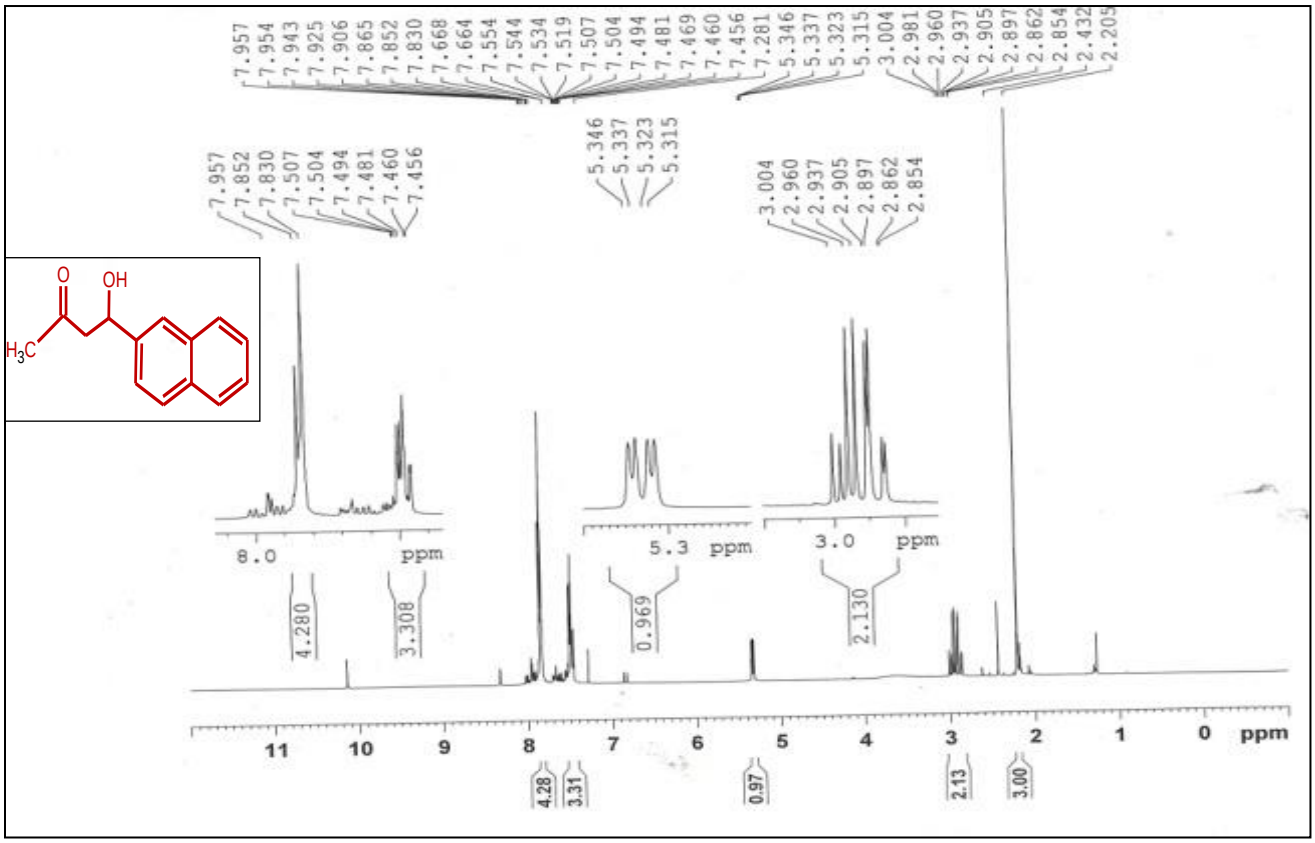

Figure 2.9(d). NMR of 4-Hydroxy-4-(2-Naphthaldehyde)butan-2-one

2.4. Conclusion

We demonstrated the use of L-proline supported ZnS nanoparticles as a catalyst for direct asymmetric aldol condensation between acetone and aldehydes. The important features of these studies are (1) the solubility problem of L-proline in acetone can be solved on supporting L-proline on ZnS nanoparticles and suspending the same in the reaction mixture. This alleviates the requirement of co-solvents like DMSO, formamide, THF etc. from the reaction. (2)The reaction is

easy to carry out at room temperature with minimum work-up at the end of the reaction; the catalyst can be easily recovered just by centrifugation/filteration. (3) The recovered catalyst can be used for several times with comparable activity. (4) On industrial scale, the direct asymmetric aldol condensation reaction can be designed on the basis of ZnS/L-proline nanoparticles. In which the reaction mixture may enter from one side of the column having fixed bed of ZnS/ L-proline nanoparticles (of definite length). The reaction mixture pass from the column for definite time, undergo reaction and chiral aldol product can be obtained from the other end of column reactor.(5) This reaction does not require any extra chiral auxiliaries to induce chirality in the product as the same can be achieved by surface coordination of L-Proline on the surface of ZnS nanoparticles.

References

[1] T.K.Hollis and B. Bosnich, *J. Am. Chem. Soc.*, 1995, **4570**,117.

[2] T. Bach, *Angew. Chem Int. Ed.*, 1994, **417**, 33.

[3] M. Ramon, *Green Chem*., 2004, **583**, 6.

[4] H.Groger, E. M. Vogel and M.Shibasaki, *Chem.Eur.J.*, 1998, **1137**, 4.

[5] B. List, D. Shabat, C. F. Barbas, III and R. A. Lerner, *Chem. Eur. J.*,1998, **881**, 4.

[6] H. J. M. Gijsen, L. Qiao, W. Fitz and C. -H. Wong, *Chem. Rev.*,1996, **443,** 96.

[7] T. Mukaiyama, K. Narasaka and K. Banno, *Chem. Lett.*, 1973, **1011**, 2.

[8] (a) D. Carmon, M. P. Lamata and L. A. Oro, *Coord. Chem. Rev.*, 2000, **200,** 717; (b) L. M. Geary and P. G. Hultin, *Tetrahedron: Asymmetry*, 2009, **131**, 20.

[9] (a) S. Kobayashi, S. Nagayama and T. Busujima, *Chem. Lett.*, 1999, **71**, 28.; *Tetrahedron*, 1999, **55**, 8739.; *J. Am. Chem. Soc.*, 1998, **8287**, 120.; (b) N. Aoyama, K. Manabe and S. Kobayashi, *Chem. Lett.*, 2004, **312**, 33.

[10] J.Jankowska, J.Paradowska and J.Mlynarski, *Tetrahedron Lett.*, 2006, **5281**, 47.

[11] J. Collin, N.Giuseppone and P. V.–Weghe, *Coord.Chem.Rev.*, 1998, **178,** 117.

[12] (a) S. E. Denmark, R. A. Stavenger and K. –T. Wong, *J. Org. Chem.*, 1998, **918**, 63; (b) S. E. Denmark and R. A. Stavenger, *Acc. Chem. Res.*, 2000, **432**, 32.

[13] T. E. Kristensen and T. Hansen, *Eur. J. Org. Chem.*, 2010, **3179**, 17.

[14] B. List, A. L. Richard and C. F. Barbas,III,*J. Am. Chem. Soc.*, 2000, **2395**, 122.

[15] L. -W. Zhao, H. –M.Shi, J. –Z.Wang and J. He, *Chem. Eur. J.*, 2012, **15323**, 18.

[16] Y. Zhou and Z. Shan,*J. Org. Chem.*, 2006, **9510**, 71.

[17]L. Hoang, S. Bahmanyar, K. N.Houk and B. List,*J. Am. Chem. Soc.*, 2003,**125**,16.

[18]M. Lakshmi Kantam, R. Thekkathu, L. Chakrapani and K. Vijaykumar,*Tetrahedron Lett.*,2008, **1498**, 49.

[19] B. M. Choudary, L. Chakrapani, T. Ramani, K. VijayKumar and M. Lakshmi Kantam, *Tetrahedron*, 2006, **9571**, 62.

[20] Z. Tang, F. Jiang, X. Cui, L. –Z. Gong, A. –Q. Mi, Y. –Z. Jiang and Y. –D. Wu, *PNAS*, 2004, **5755**, 101.

[21]A. Lu, T. P. Smart, T. H. Epps III, D. A. Longbottom and R. K. O'Reilly, *Macromolecules*,2011, **7233**, 44.

[22]R. L. Sutar and N. N. Joshi, *Tetrahedron:Asymmetry*, 2013, **43**, 24.

[23]X. Z. Tang, F. Jiang, X. Cui, L.-Z. Gong, A.-Q.Mi, Y.-Z. Jiang and Y.-D. Wu, *PNAS*,2004, **5755**, 101.

[24] R. Jenkins and R.L. Snyder, Introduction to X-Ray Powder Diffractometry, John Wiley and Sons, NewYork, 1996.

[25] R. Rossetti, R. Hull, J.M. Gibson and L.E. Brus, *J. Chem. Phys.*,1985, **552**, 82.

[26] A. Goudarzi, G. M. Aval, S. S. Park, M. C. Choi, R.Sahraei, M. H. Ullah, A. Avane and C. S. Ha, *Chem. Mater.*, 2009, **2375**, 21.

[27] W. G. Becher and A. J. Bard, *J. Phys. Chem.*, 1983, **4888**, 87.

[28] B. M. Trost and H. Ito, *J. Am. Chem. Soc*., 2000, **12003**, 122.

[29]B. M. Trost, H. Ito and E. R. Silcoff, *J. Am. Chem. Soc.*, 2001, **3367**, 123.

[30]A. Barth,Prog.*Biophys. Mol. Biol.*, 2000, **141**, 74.

[31]A. R. Garcia, B. R. deBarros, J. P. Lourence and L. M. Ilhara,*J. Phys. Chem. A.*, 2008, **8280**, 112.

[32]M. Kakihana, T. Nagumo, O. Makoto and H. Kakihana, *J.Phys.Chem.*,1987, **6128**, 91.

[33] P. Jeevanandam and K. J. Klabunde, *Langmuir*, 2002, **5309**, 18.

[34] DMSO Health and Safety Information Bulletin, 2007, **106**.

[35] S. D. Naik and L. K. Doraiswamy, *AIChE J.*,1998, **612**, 4.

[36] D. Seebach, M. Boes, R. Waef and W. B. Schweizer, *J. Am. Chem. Soc.*, 1983, **5390**, 105.

[37] F. Orsini, F.Pelizzoni, M. Forte, R. Destro and P. Cariboldi, *Tetrahedron*, 1988, **519**, 44.

[38] A. Basson, W. Zou, E. Reyes, F. Himo and A. Cordova, *Angew. chem. Int. Ed.*, 2005, **7028**, 44.

[39] F.R. Clemente and K. N.Houk,*Angew. Chem. Int. Ed.*, 2004, **5766**, 43.

[40] S. Bahmanyar and K. N. Houk,*J. Am. Chem. Soc.*, 2001, **11273**, 123.